

The divergence as $L \rightarrow \infty$ in the first term on the right-hand side of eq A9 (which is propagated to $\Phi_{\text{EXT}}^L(r_j)$ in eq A5, and ultimately to $U_{\text{EXT}}^L(r_j)$) is exactly canceled by the divergence in the first term on the right-hand side of eq A4. Thus, eq 1 is left as the contribution to the total configuration energy from the interaction between ion j and an infinite cylindrical polyion of charge density $-q/b$, and eq 6 can be used to calculate $\Phi_{\text{EXT}}(r_j)$.

The accuracy of the numerical determination of $\Phi_{\text{EXT}}^L(r_s)$ from eq A6 and A9 is limited primarily by the magnitude of Δr , the thickness over which $B(r_s, r_s; L)$ and hence $\Phi_{\text{EXT}}^L(r_s)$ are assumed to be constant. Values of Δr less than the standard choice of 0.1 nm were tested and found to produce no significant alteration in the counterion distribution computed for salt-free systems. However, at ratios of added salt to polyion monomer ($[\text{Na}]/[\text{P}]$) in excess of two, anomalous local inversions were observed in the computed distributions of the counterions and co-ions near the outer boundary (R) of the MC cell. Similar "spurious boundary effects" apparently were observed by Rossky and co-workers,¹⁸ who stressed the importance of high accuracy in the numerical evaluation of the external potential. Anomalies in the ion distribution near R were reduced (but not eliminated) by use of smaller values of the grid size Δr (0.05 nm, 0.025 nm) and/or by increasing the length of the central cell beyond 1.7 nm. For systems containing added salt, the external potential was not in general computed with the SC method, because of the limited storage capability of the computer (Harris/7). Calculation of Φ_{EXT} from the PB equation, which has been previously employed to approximate long-range interactions in MC studies,^{10,16} significantly reduces the demands of these simulations on the computer memory. Therefore, the ion distributions in added salt reported in section V all were calculated from the PB external potential

$$\Phi_{\text{EXT}}^{\text{PB}}(r_s) = (2/\epsilon) \sum_{s'=1}^S B(r_s, r_{s'}; L) \int_{r_s}^{r_s+\Delta r} \rho^{\text{PB}}(r) r dr \quad (\text{A10})$$

where $\rho^{\text{PB}}(r)$ is the net charge density predicted by the cylindrical PB equation, the grid size $\Delta r = 0.5$ nm, and $2h = 1.7$ nm. To check the accuracy of this use of the PB equation in the MC simulations, the resulting ion distributions for a system with $[\text{Na}]/[\text{P}] = 2.0$ were compared with those computed by using the SC method to determine $\Phi_{\text{EXT}}(r_j)$. The ion distributions obtained by these two methods are indistinguishable. Consequently, for systems containing higher levels of added salt

($[\text{Na}]/[\text{P}] > 2.0$), where the effects of long-range interactions must be less significant, the PB equation was deemed to provide a sufficiently accurate alternative to the SC method of computing the external potential. The residual charge inversion near R (cf. Figure 5) is not expected to have any impact on the results discussed in section V, which is focused on the characteristics of the counterion distribution function in the near vicinity of the polyion.

In contrast to the methods described above for calculating the contribution of long-range interactions to the total configuration energy, the extended image (EI) method does not involve the calculation of an averaged external potential. Instead, all interactions among small ions within the central cell and all interactions of each of these ions with all of the ions in all the "image cells" are calculated explicitly. The potential energy of the interaction between ion j in the central cell (denoted by the subscript 0) and ion k , which may be in the central cell or in any of the m image cells, is

$$U_{j0,km} = q_{j0}q_{km}/\epsilon|\bar{r}_{j0} - \bar{r}_{km}| \quad m = 0, \dots, M; j, k = 1, \dots, N \quad (\text{A11})$$

provided that $|\bar{r}_{j0} - \bar{r}_{km}| \geq \delta$, the hard-sphere cutoff. To diminish correlations in the angular coordinates of the image ions with those of ions in the central cell, each odd-indexed image cell was rotated by 180° , so that

$$|\bar{r}_{j0} - \bar{r}_{km}| = [(x_{j0} - (-1)^m x_{km})^2 + (y_{j0} - (-1)^m y_{km})^2 + (z_{j0} - (z_{k0} + 2mh))^2]^{1/2}$$

(This approach was taken by LeBret and Zimm¹⁷ in their MC computations of ion distributions around DNA.) If the model polyion is assumed to have a continuous axial charge distribution, then the EI expression for the total configuration energy is

$$E_{\text{TOT}}^L = \sum_{j=1}^N U_{\text{ps}}^{\text{con}}(r_j, L) + \frac{1}{2} \sum_{j=1}^N \sum_{k=1}^N U_{j0,k0} + 2 \sum_{j=1}^N \sum_{k=1}^N \sum_{m=1}^M U_{j0,km} \quad (\text{A12})$$

This form of the configuration energy was assumed in applying the EI method to compute the values of $\beta_{\text{con}}(0.1)$ given in Table I for various specifications of $2h$ and L . (All of these computations based on the EI method were carried out by K. Kollenbrander and L. Bleam.³²)

(32) Kollenbrander, K. Senior Thesis, Central College, IA, 1983.

Collisional Model for Diatomic Recombination Reactions[†]

Michal Borkovec and Bruce J. Berne*

Department of Chemistry, Columbia University, New York, New York 10027 (Received: February 25, 1985; In Final Form: April 8, 1985)

We evaluate the dissociation or recombination rate constant of a diatomic molecule using the impulsive collisional BGK model. In three dimensions the rate constant goes through a maximum as a function of the collision rate as in the case of isomerization reactions. For high collision rate it reduces to the classical Smoluchowski result for diffusion-controlled reactions. This model quantitatively fits experimental data on halogen recombination. The experimentally observed maximum has its dynamical origin in the competition of collisional activation and diffusion control as originally suggested by Kramers.

1. Introduction

Chemical reactions have been studied extensively within the framework of unimolecular rate theory in the gas phase^{1,2} and the theory of diffusion-controlled reactions³ in liquids. More general models based on Kramers' ideas⁴ can be applied over the whole density range. Theoretical studies of isomerization reactions

using similar models⁵⁻⁹ show that the rate constant as a function of the coupling parameter (e.g., friction or collision rate) goes

(1) Troe, J. *Annu. Rev. Phys. Chem.* 1978, 29, 223. Haase, W. L. In "Modern Theoretical Chemistry"; Miller, W. H., Ed.; Plenum Press: New York, 1976; Vol. 2B. Luther, K.; Troe, J. In "Reactions of Small Transient Species"; Fontijn, A.; Clyne, M. A. A., Eds.; Academic Press: New York, 1983.

(2) Troe, J. *J. Chem. Phys.* 1977, 66, 4745.

[†]This research was supported by a grant from NSF.

through a characteristic maximum (turnover). Prompted by this theoretical work there was a substantial effort to observe this turnover experimentally.^{10,11} Even though such studies provided many interesting results a turnover was reported only in the case of cyclohexane isomerization.¹⁰ In this case however the important equilibrium solvent effect is hard to estimate quantitatively and the potential surface of cyclohexane is not accurately known. Comparison of the experimental data with dynamical theories is therefore problematic.⁵

It is surprising that in spite of these difficulties the interest focused solely on isomerization reactions. Dissociation and recombination reactions were never considered in this context even though it has been known for a decade that the rate constant of halogen recombination shows a turnover as a function of pressure.¹²⁻¹⁴ Therefore, one would like to compare these results with a physically interesting model of dissociation or recombination reactions valid for arbitrary coupling.

In this study we consider one such model: the impulsive collisional BGK model having collision rate as the coupling parameter.^{6,7} For low coupling the BGK model resembles the "strong collision approximation" known in unimolecular rate theory.¹ At high coupling it shows the physically correct diffusive behavior. We evaluate explicitly the rate constant for dissociation or recombination as a function of the collision rate. The rate constant shows the characteristic turnover and reduces correctly to the Smoluchowski diffusion-controlled recombination rate constant for high coupling. Troe's experiments on halogen recombination^{12,13} can be explained by using this model. The analogous study of the original Kramers' frictional model is more complicated and is considered in a separate publication.¹⁵

2. Definition of the Model

Consider the simplest dissociation reaction



where the two atoms are separated by \vec{r} and carry a relative momentum \vec{p} . The classical Hamiltonian in the phase space Γ is¹⁶

$$H(\Gamma) = p_r^2/2\mu + V_{\text{eff}}(r, J) \quad (2)$$

where p_r is the radial component of the momentum, μ is the reduced mass, and

$$V_{\text{eff}}(r, J) = V(r) + J^2/2\mu r^2 \quad (3)$$

is the effective rotational potential. The atoms interact by a potential $V(r)$ which approaches the constant dissociation energy D_e (faster than $1/r^2$) for large r . The effective potential $V_{\text{eff}}(r, J)$ as function of r has a maximum which depends on the angular momentum J .¹⁶

Reactants and products are defined by a characteristic function

(3) Calef, D.; Deutch, J. M. *Annu. Rev. Phys. Chem.* **1983**, *34*, 493.

(4) Kramers, H. A. *Physica (Utrecht)* **1940**, *7*, 284.

(5) Carmeli, B.; Nitzan, A. *J. Chem. Phys.* **1984**, *80*, 3596.

(6) Skinner, J. L.; Wolyne, P. G. *J. Chem. Phys.* **1980**, *72*, 4913; **1978**, *69*, 2143. Berne, B. J.; Skinner, J. L.; Wolyne, P. G. *J. Chem. Phys.* **1980**, *73*, 4314.

(7) Montgomery, J. A.; Chandler, D.; Berne, B. J. *J. Chem. Phys.* **1979**, *70*, 4065.

(8) Grote, R. F.; Hynes, J. T. *J. Chem. Phys.* **1980**, *73*, 2715. Hänggi, P.; Weiss, U. *Phys. Rev. A* **1984**, *29*, 2265.

(9) Hänggi, P.; Moitabai, F. *Phys. Rev. A* **1982**, *26*, 1168. Hänggi, P. *J. Stat. Phys.* **1983**, *30*, 401. Bagchi, B.; Oxtoby, D. W. *J. Chem. Phys.* **1983**, *78*, 2735.

(10) Hasha, D. L.; Eguchi, T.; Jonas, J. *J. Am. Chem. Soc.* **1982**, *104*, 2290.

(11) Rothenberger, G.; Negus, D. K.; Hochstrasser, R. M. *J. Chem. Phys.* **1983**, *79*, 5360. Velsko, S. P.; Waldeck, D. H.; Fleming, G. R. *J. Chem. Phys.* **1983**, *78*, 249. Courtley, S. H.; Fleming, G. R. *J. Chem. Phys. Lett.* **1984**, *103*, 443. Eissenthal, K.; Millar, A., preprint. Eissenthal, K., private communication.

(12) Otto, B.; Schoeder, J.; Troe, J. *J. Chem. Phys.* **1984**, *81*, 202.

(13) Hippler, H.; Schubert, V.; Troe, J. *J. Chem. Phys.* **1984**, *81*, 3931.

(14) Hippler, H.; Troe, J. *Int. J. Chem. Kinet.* **1976**, *8*, 501.

(15) Borkovec, M.; Berne, B. J., in preparation.

(16) Goldstein, H. "Classical Mechanics"; Addison-Wesley: Reading, MA, **1981**; Chapter 3.

$$H_{AB}(r) = \theta(r_{\text{TST}} - r) \quad (4)$$

where $\theta(x)$ is the Heaviside step function. $H_{AB}(r)$ is 1 for a bound diatomic molecule and vanishes for dissociated atoms. We denote by r_{TST} the fixed position of the transition-state dividing surface (see section 3).

Consider now a collection of AB molecules interacting with a heat bath of interest (i.e., the solvent). We are interested in the dynamics of the decay of some initial nonequilibrium macroscopic state to equilibrium. Although this problem is severely complicated by many-body effects^{3,17} the dynamics in three dimensions can be approximated quite accurately by the solution of the standard chemical kinetic equations involving the dissociation and recombination rate constants $k^{(d)}$ and $k^{(r)}$.^{3,18}

We evaluate the dissociation rate constant $k^{(d)}$ using the following idea: let us imagine that we modify our potential $V(r)$ by putting a hard wall at $r = L$ ($L \gg r_{\text{TST}}$). Then there is no difference between this reaction and an isomerization reaction whose forward and backward rate constants are obtained from the equilibrium constant and the correlation time of the correlation function^{7,19}

$$C(t) = \langle \delta H_{AB}(t) \delta H_{AB}(0) \rangle \quad (5)$$

where δH_{AB} denotes the deviation of H_{AB} from equilibrium value and $\langle \dots \rangle$ the canonical equilibrium average over full space ($0 \leq r \leq L$). Using this modified potential we calculate the forward rate constant from this formalism. If the limit $L \rightarrow \infty$ of this rate constant exists we assume that the forward rate constant is equal to the dissociation rate constant $k^{(d)}$ of eq 1.

Once $k^{(d)}$ is determined the recombination rate constant $k^{(r)}$ of eq 1 follows from detailed balance.

$$K_{\text{eq}} = k^{(d)}/k^{(r)} \quad (6)$$

The equilibrium constant is²⁰

$$K_{\text{eq}} = e^{-\beta D_e}/Z_{AB} \quad (7)$$

where $\beta = 1/k_B T$ and

$$Z_{AB} = \int d^3 r e^{-\beta V(r)} H_{AB}(r) \quad (8)$$

the configurational partition function of the bound diatomic.

In this communication we study the dissociation rate constant $k^{(d)}$ for the simple collisional BGK model acting on the relative coordinates. The transition rate is characterized by a collision kernel^{6,7}

$$K(\Gamma'|\Gamma) = \alpha \delta(\vec{r}' - \vec{r}) P_{\text{eq}}(\vec{p}') \quad (9)$$

where $P_{\text{eq}}(\vec{p})$ is the Maxwell-Boltzmann distribution. The collisions of mean frequency α randomize the momentum \vec{p} but not the position \vec{r} . This corresponds physically to the case of most favorable energy transfer by a heavy hard collider.

3. Evaluation of the Dissociation Rate Constant

Unfortunately, it is not possible to evaluate the dissociation rate constant $k^{(d)}$ for arbitrary collision rate α analytically. However, this becomes feasible in three limiting cases, and these results can be used to approximate accurately the overall behavior.

The dynamics of the isolated molecule determines the maximal rate constant which is given by transition-state theory. It can be evaluated from the initial slope of the correlation function $C(t)$.¹⁹ In our case we obtain a dissociation rate constant

$$k_{\text{TST}}^{(d)} = \langle H_{AB} \rangle^{-1} \langle \delta(r_{\text{TST}} - r) (p_r/\mu) \theta(p_r) \rangle \quad (10)$$

(17) Kapral, R. *Adv. Chem. Phys.* **1981**, *48*, 71.

(18) Zumofen, G.; Blumen, A.; Klafter, J. *J. Chem. Phys.*, in press. Anacker, L. W.; Kopelman, R. *J. Chem. Phys.* **1984**, *81*, 6402.

(19) Chandler, D. *J. Chem. Phys.* **1978**, *68*, 2959. Berne, B. J. In "Multiple Time Scales"; Brackbill, J. U., Cohen, B. I., Eds.; Academic Press: New York, in press.

(20) McQuarrie, D. A. "Statistical Mechanics"; Harper & Row: New York, 1976.

giving

$$k_{\text{TST}}^{(d)} = \frac{1}{Z_{\text{AB}}} \left(\frac{8\pi}{\beta\mu} \right)^{1/2} r_{\text{TST}}^2 e^{-\beta V(r_{\text{TST}})} \quad (11)$$

which still depends on the unknown location of the transition-state r_{TST} . For a given potential and temperature r_{TST} is found by minimizing the transition-state rate constant eq 11 with respect to r_{TST} . This definition of the transition state is in the spirit of the canonical variational transition-state theory.²¹

In the low-collision limit the BGK model is a "strong collision" model because it allows large changes in energy and angular momentum during one collision.^{6,22} The dissociation rate constant can be evaluated by standard techniques from unimolecular rate theory²

$$k_{\text{low}}^{(d)} = \int_{Q(J) < E} d\vec{J}' dE' \int_{Q(J) > E} d\vec{J} dE K(E', \vec{J}' | E, \vec{J}) P_{\text{eq}}(E, \vec{J}) \quad (12)$$

where $K(E', \vec{J}' | E, \vec{J})$ is the average single collisional transition rate from E, \vec{J} to E', \vec{J}' and $P_{\text{eq}}(E, \vec{J})$ the equilibrium distribution of the total energy E and angular momentum \vec{J} . $Q(J)$ is the dissociation threshold, i.e., the value of $V_{\text{eff}}(r, J)$ at its maximum for a given angular momentum \vec{J} . The procedure which was used to evaluate this expression for constant Q previously²² can be followed in this case. The transition rate $K(E', \vec{J}' | E, \vec{J})$ is obtained by averaging eq 9 over a "microcanonical" ensemble with constant E and \vec{J} . This is inserted into eq 12 which yields the dissociation rate constant

$$k_{\text{low}}^{(d)} = \alpha \frac{\langle \theta(D_e - V(r)) h(\vec{r}) (1 - h(\vec{r})) \rangle}{\langle \theta(D_e - V(r)) h(\vec{r}) \rangle} \quad (13)$$

where

$$h(\vec{r}) = \int d\vec{p} P_{\text{eq}}(\vec{p}) \theta(Q(J(\Gamma)) - H(\Gamma)) \quad (14)$$

All canonical averages have to be restricted to the region of phase space where the diatomic cannot dissociate.²² Note that this low-pressure rate constant $k_{\text{low}}^{(d)}$ is proportional to the collision frequency α . It can be shown that this expression is very similar to the result of the "strong collision approximation".

In the high collision rate limit, the BGK model can be described by a diffusion equation in position space with a diffusion coefficient^{6,7}

$$D = 1/\beta\mu\alpha \quad (15)$$

Unfortunately, in this case the popular mean first passage time approach gives a divergent result as $L \rightarrow \infty$ so that we must evaluate the correlation time of eq 5 with more caution. The correlation time of a quantity $A(r)$ with zero mean and unit variance can be obtained as follows.²³ First one has to solve the adjoint of the Smoluchowski diffusion equation

$$D r^2 \frac{d}{dr} \left(r^2 \frac{dT(r)}{dr} \right) - \beta D \frac{dV(r)}{dr} \frac{dT(r)}{dr} = -A(r) \quad (16)$$

for $T(r)$ with reflecting boundary condition at $r = 0$ and absorbing boundary condition at $r = L$. The correlation time is then obtained by averaging $A(r) T(r)$ over full space ($0 \leq r \leq L$). In this case

$$A(r) = \frac{H_{\text{AB}}(r) - \langle H_{\text{AB}} \rangle}{(\delta H_{\text{AB}}^2)^{1/2}} \quad (17)$$

where the equilibrium averages are evaluated over the full space ($0 \leq r \leq L$). Relating the correlation time to the dissociation rate constant¹⁹ we obtain in the limit $L \rightarrow \infty$

$$k_{\text{high}}^{(d)} = D \left\{ \int_0^\infty dr P(r) H_{\text{AB}}(r) \int_r^\infty dr' P^{-1}(r') \int_0^{r'} dr'' P(r'') H_{\text{AB}}(r'') \right\}^{-1} \quad (18)$$

where

$$P(r) = \frac{1}{Z_{\text{AB}}} 4\pi r^2 e^{-\beta V(r)} \quad (19)$$

For deep wells this expression together with eq 6 becomes equivalent to the classical Smoluchowski result for diffusion-controlled recombination rate constant³ (see sections 4 and 5). This rate constant is inversely proportional to the collision frequency α .

We have now evaluated $k^{(d)}$ in three different limiting cases. An expression valid approximately for any collision rate α is obtained by considering a Pade-like approximant for $k^{(d)}$ (or $k^{(r)}$)

$$k^{-1} \simeq k_{\text{low}}^{-1} + k_{\text{TST}}^{-1} + k_{\text{high}}^{-1} \quad (20)$$

which can be viewed as the sum of mean times for each particular mechanism. The use of this formula should not be limited to the particular situation considered here. Similar expressions have been proposed recently.⁸ Analogues of eq 20 with two terms enjoy popular use in reaction dynamics.^{1-3,6,12,17} We justify eq 20 by comparing with simulation data in the next section.

4. Comparison with Simulations

For the simple potential

$$V(r) = D_e \theta(r - a) \quad (21)$$

one can evaluate $k^{(d)}$ for large dissociation energies D_e explicitly. Using eq 6-8 we obtain for the transition-state recombination rate constant

$$k_{\text{TST}}^{(d)} = a^2 \left(\frac{8\pi}{\beta\mu} \right)^{1/2} \quad (22)$$

which is the free molecular limit.^{17,24} In the low collision limit ($\alpha \rightarrow 0$) one obtains similarly from eq 13

$$k_{\text{low}}^{(r)} \sim 4\alpha a^3 \left(\frac{\pi}{\beta D_e} \right)^{1/2} \quad (23)$$

which coincides with the result obtained from the "strong collision approximation". In the diffusive limit ($\alpha \rightarrow \infty$) one obtains from eq 18

$$k_{\text{high}}^{(r)} \sim 4\pi D a \quad (24)$$

the familiar Smoluchowski result for diffusion-controlled reactions.³ The rate constant for arbitrary collision rate can be obtained by inserting eq 22-24 into eq 20.

We have performed computer simulations to address the validity of the Pade-like approximant eq 20. We follow trajectories in the potential eq 21 which suffer BGK collisions with mean frequency α .⁷ The particle has been enclosed in a reflecting sphere of radius $L \gg a$. The reactive flux was obtained by averaging $\theta(a - r)$ as described previously.⁷ In the high collision region the trajectories have to be followed until all nonreactive modes decay (a few hours on a VAX 11/780). A set of simulation results for $L = 50a$ and $\beta D_e = 5$ is presented in Figure 1. The full line is eq 20 using the corresponding exact results instead of eq 22-24 where necessary. We see that the agreement with eq 20 is indeed satisfactory.

5. Comparison with Experiments

Recently recombination rate constants of iodine were reported as a function of the diffusion coefficient of a single iodine atom, D_I , which was varied by changing the pressure.¹² To compare this data with the BGK model we use the Morse potential

$$V(r) = D_e (1 - e^{-b(r-r_e)})^2 \quad (25)$$

where $b = (\mu\omega_0^2/2D_e)^{1/2}$ to model the interaction between iodine atoms. The parameters $D_e = 1.555$ eV, $\omega_0 = 4.04 \times 10^{13}$ s⁻¹, $r_e = 2.66$ Å, and $\mu = 63.5$ g/mol were taken from spectroscopic

(21) Truhlar, D. G.; Garrett, B. C. *Annu. Rev. Phys. Chem.* **1984**, *35*, 159.

(22) Borkovec, M.; Berne, B. J. *J. Chem. Phys.* **1985**, *82*, 794.

(23) Szabo, A.; Schulten, K.; Schulten, Z. *J. Chem. Phys.* **1980**, *72*, 4350.

(24) Sahni, D. C. *Phys. Rev. A* **1984**, *30*, 2056. Wagner, P. E.; Kerker, M.; *J. Chem. Phys.* **1977**, *66*, 638.

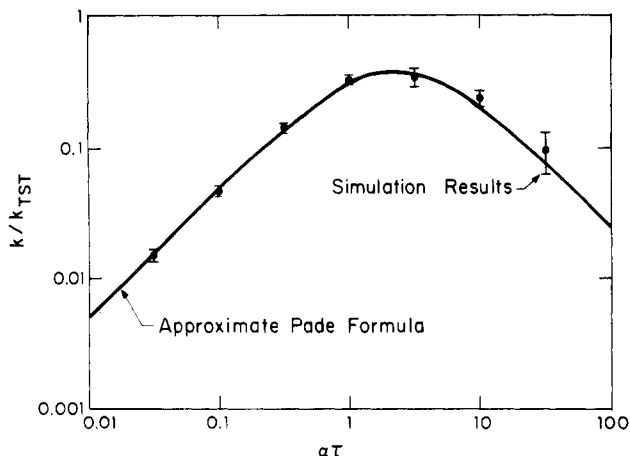


Figure 1. Comparison of simulation data with the approximate analytical expression eq 20. The rate constant k is plotted vs. the collision rate α in dimensionless units where $\tau = (\mu\alpha^2\beta)^{1/2}$. The error bars represent 95% confidence intervals.

tables.²⁵ The collision rate α was chosen to reproduce the relative diffusion coefficient eq 15 of the two iodine atoms which is $D = 2D_1$ in the dilute solution in question. Using eq 6–8 we can reduce the diffusion-controlled recombination rate constant eq 18 (for deep wells) to the correct result for interacting particles³

$$k_{\text{high}}^{(r)} \sim 4\pi D \left\{ \int_{r_c}^{\infty} dr \frac{e^{\beta U(r)}}{r^2} \right\}^{-1} \quad (26)$$

where $U(r) = V(r) - D_c$. The evaluation of eq 11, 13, and 26 requires simple numerical analysis. The transition-state rate constant eq 11 must be reduced by a factor of $1/2$ to take the indistinguishability of the iodine atoms into account.²⁶ The transition state is located at $r_{\text{TST}} = 3.51 \text{ \AA}$ in this particular example. Then we use eq 20 to obtain the rate constant for any diffusion coefficient. Note that there are *no* adjustable parameters. The result is displayed together with experimental data¹² in Figure 2. The two different temperatures of measurements (298 and 314 K) produced virtually identical graphs.

6. Conclusions

We have evaluated the dissociation or recombination rate constant for a classical diatomic molecule as a function of collision rate for the impulsive collisional BGK model. It is possible to calculate the rate constant analytically in three limiting cases. These quantities are sufficient to construct approximately the overall rate constant (see Figure 1 for comparison with simulation). In the high coupling limit we correctly obtain the Smoluchowski result for diffusion-controlled reactions. This model was applied to interpret Troe's recent measurements¹² of recombination rate constants of iodine over a wide density range. The result which does not contain any adjustable parameters is compared with experimental data in Figure 2. The experimentally observed maximum has its dynamical origin in the competition of collisional activation and diffusion control as proposed originally by Kramers.⁴

We would like to emphasize the importance of the correct number of the degrees of freedom which enter the model: the diffusion-controlled regime for a dissociation reaction behaves completely differently in one²⁷ and two²⁸ dimensions in contrast to three dimensions treated here. In these cases the analogues of eq 18 diverge in the $L \rightarrow \infty$ limit.

Despite the agreement between theory and experiment the quantitative success of the BGK model should be judged with caution. The model involves many approximations which are

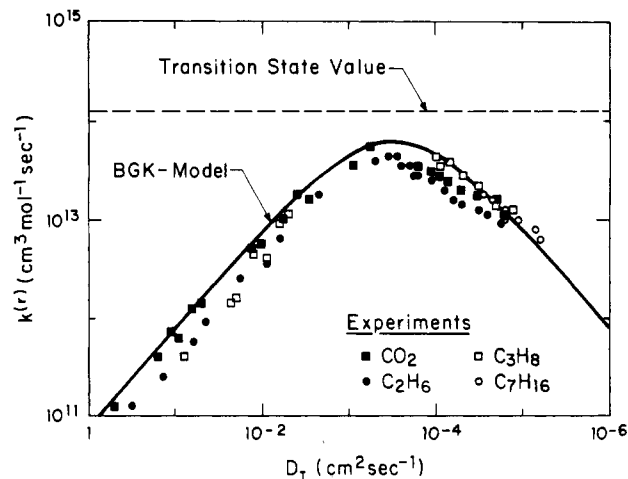


Figure 2. Troe's experimental data of recombination rate constants $k^{(r)}$ of iodine as function of the diffusion coefficient of a single iodine atom, D_1 , in different solvents (dots);¹² the prediction of the impulsive collisional BGK model without adjustable parameters (full line) and the value of the transition-state rate constant (dashed line).

presumably justified for higher pressures only. The precise quantitative agreement in the low-pressure region is probably fortuitous. We will discuss the approximations which enter the BGK model in the order of decreasing importance.

(1) From the trajectory studies²⁹ of $2A + B \rightarrow A_2 + B$ type reactions in the low-pressure regime it is known that two reaction channels are of importance: the bound complex (BC mechanism²⁹) and the energy-transfer mechanism (ET mechanism²⁹) considered in this study. In the BC mechanism a host gas molecule forms a complex with one of the recombining radicals which can form the products upon a collision with a second radical. This reaction channel becomes dominant at lower temperatures ($\sim 300 \text{ K}$) and is responsible for the experimentally observed³⁰ decrease of the low-pressure recombination rate constant with temperature (roughly as T^{-3}). The ET mechanism corresponds to energy activation and deactivation of the reacting molecule by the inert gas molecules and becomes important at high temperatures ($\sim 1000 \text{ K}$).²⁹ This ET mechanism is described by the BGK model for example. Trajectory calculations²⁹ show that the rate constant of the ET mechanism decreases weakly with temperature (slower than T^{-1}). Using the Lennard-Jones expression for the diffusion coefficient²⁰ or the true collision frequency² the BGK model predicts a too large recombination rate constant with no temperature dependence. This is not surprising however since the BGK model corresponds to the maximum possible energy transfer. In reality the energy transfer will be much less efficient and described rather by a weak-collision model which results in a smaller rate constant which decreases with temperature. The original Kramers model applied to this particular problem¹⁵ shows roughly a correct temperature dependence (close to $T^{-1/2}$). However, a realistic model must take the non-Markovian nature of soft collisions into account.

(2) We have to address the electronic degeneracy factors σ included usually in more accurate studies^{29,31} but omitted in our model for simplicity. The ground state of iodine atom is $^2P_{3/2}$ (4-fold degenerate) and the ground state of the iodine molecule is $^1\Sigma_g^+$ (nondegenerate).²⁵ If the reaction proceeds adiabatically (slow intersystem crossing) the recombination rate constant will be reduced by a factor of $\sigma = 1/16$. However if the reaction is nonadiabatic (fast intersystem crossing) all electronic states lead to recombination and $\sigma = 1$. A continuous transition is to be

(25) Herzberg, G. "Molecular Spectra and Molecular Structure", 2nd ed.; Van Nostrand: New York, 1950; Vol. I.

(26) Pechukas, P. In "Modern Theoretical Chemistry"; Miller, W. H., Ed.; Plenum Press: New York, 1976; Vol. 2B.

(27) Torney, D. C.; McConnell, H. M. *J. Phys. Chem.* **1983**, *87*, 1941.

(28) Keizer, J. *J. Phys. Chem.* **1981**, *85*, 940.

(29) Clarke, A. G.; Burns, G. *J. Chem. Phys.* **1972**, *56*, 4636. Chang, D. T.; Burns, G. *Can. J. Chem.* **1976**, *54*, 1535.

(30) Boyd, R. K.; Burns, G. *J. Phys. Chem.* **1979**, *83*, 88. Blake, J. A.; Burns, G. *J. Chem. Phys.* **1971**, *54*, 1480. Ip, J. K. K.; Burns, G. *J. Chem. Phys.* **1972**, *56*, 3155. Antrim, R. E.; Burns, G.; Ip, J. K. K. *Can. J. Chem.* **1977**, *55*, 749.

(31) Stace, A. J.; Murrell, J. N. *Mol. Phys.* **1977**, *33*, 1.

expected between these extreme situations depending on the ratio of the intersystem crossing times to the lifetimes of closely separated radicals during recombination. It is established that in radicals the hyperfine (hf) interactions are the major mechanism for intersystem crossing.³² In halogen atoms the time scale for intersystem crossing will probably lie in the picosecond range (hf-coupling constants $\sim 10^4$ G³³). Usually in organic radicals this time scale is of the order of nanoseconds (hf-coupling constants ~ 10 G).³² In the case of halogen atoms one therefore expects $\sigma = 1/16$ in the low-pressure region because the duration of one collision is too short for recrossing. Rate constants obtained from trajectory studies without adjustable parameters ($T \approx 300$ K) come out too low with $\sigma = 1/16$.^{29,31} This could be explained either by recrossings in long-lived collision complexes which move on weakly attracting potential surfaces or by inaccuracies in the potential surfaces used in the trajectory studies. In the diffusive regime on the other hand the radicals stay close to each other for the lifetime of solvent cage (i.e., the time of diffusional escape) which is in the picosecond range. This allows enough time for intersystem crossing leading to $\sigma = 1$ in the high-pressure regime for iodine recombination. On the other hand in organic radical reactions $\sigma < 1$ is experimentally observed³⁴ even in the diffusive regime. This is naturally explained by the long intersystem crossing times.

(3) We approximate the interaction between the iodine atoms by a Morse potential at all densities. Since the calculated rate constants are not too sensitive to changes of the parameters entering the Morse potential we believe that this is adequate at low pressure. A more stringent test would involve the study of different functional forms of the potential which we omitted in light of the more serious approximations stated above. Furthermore, as one increases the density the reactants feel the solvent-averaged potential of mean force. Since the species in question are unpolar the magnitude of this solvent effect can be estimated by approximating the potential of mean force using the cavity distribution function of hard spheres.³⁵ Tabulated Lennard-Jones

parameters can be used to obtain the hard-sphere diameters. We find only minor changes ($\sim 10\%$) in the diffusive rate constant³⁶ and in the transition-state rate constant. Therefore, we feel that this effect is probably of minor importance in this particular case.

We also applied the same model on data for bromine¹³ and chlorine¹⁴ recombination. The data obtained on bromine are very similar to those on iodine and show also a good agreement with the BGK model. We are puzzled by chlorine however where the turnover appears at substantially lower densities than in iodine or bromine and is in disagreement with the BGK model.

The density dependence of the recombination of polyatomic molecules or radicals can be analyzed by similar methods. Because of the large number of degrees of freedom involved one has to expect much larger low-pressure rate constants in this case.^{1,22} In this case the maximum of the rate constant vs. pressure will be substantially broadened and shifted toward lower pressures. Therefore, experimental study of such recombination reactions over a wide pressure range could supplement the studies on isomerization reactions. It would also be interesting to perform such studies in very viscous solvents. In organic radical reaction one might observe the approach of the electronic degeneracy factor σ to 1 with increasing viscosity. Also non-Markovian effects on the diffusive falloff as considered in isomerization reactions^{5,8,9} could be addressed in recombination reactions.

In conclusion we summarize the most important results. We have evaluated the rate constant for the dissociation or recombination of a diatomic using the impulsive collisional BGK model for arbitrary coupling. The rate constant as a function of the collision rate goes through a maximum and reduces to the classical Smoluchowski result for diffusion-controlled reactions for high collision rate. The simple BGK model is able to reproduce the recent measurements of iodine recombination by Troe¹² without adjustable parameters (see Figure 2). The physical reason for the turnover observed by Troe has the dynamical origin in the competition between collisional activation and diffusion control as originally suggested by Kramers.⁴

Acknowledgment. We thank Professor P. Pechukas, Dr. D. Thirumalai, J. Straub, and M. Zimmt for helpful discussions.

(32) Molin, Yu N., Ed. "Spin Polarization and Magnetic Effects in Radical Reactions"; Elsevier: Amsterdam, 1984. Kapstein, R. In "Chemically Induced Magnetic Polarization"; Muus, L. T., Atkins, P. W., McLauchlan, K. A., Pedersen, J. B., Eds.; D. Reidel: Boston, 1977.

(33) Hudson, A.; Root, K. D. *J. Adv. Magn. Reson.* **1971**, *5*, 1.

(34) Lipscher, J.; Fisher, H. *J. Phys. Chem.* **1984**, *88*, 2555. Schuh, H.; Fischer, H. *Int. J. Chem. Kinet.* **1976**, *8*, 341.

(35) Pratt, L. R.; Hsu, C. S.; Chandler, D. *J. Chem. Phys.* **1978**, *68*, 4202. Ladanyi, B. M.; Evans, G. T. *J. Chem. Phys.* **1983**, *79*, 944.

(36) Hynes, J. T.; Kapral, R.; Torrie, G. M. *J. Chem. Phys.* **1980**, *72*, 177. Northrup, S. H.; Hynes, J. T. *J. Chem. Phys.* **1979**, *71*, 871.